Case Studies in Thermal Engineering 28 (2021) 101494

Contents lists available at ScienceDirect

Case Studies in Thermal Engineering

journal homepage: www.elsevier.com/locate/csite

Experimental investigation of heat transfer performance of novel bio-extract doped mono and hybrid nanofluids in a radiator

Kelvin U. Efemwenkiekie [a], Sunday O. Oyedepo [a,*], Solomon O. Giwa [b], Mohsen Sharifpur [c,d,**], Taiwo F. Owoeye [e], Kehinde D. Akinlabu [e], Josua P. Meyer [c]

[a] Department of Mechanical Engineering, Covenant University, Ota, Nigeria
[b] Department of Mechanical Engineering, Olabisi Onabanjo University, Ogun State, Nigeria
[c] Department of Mechanical and Aeronautical Engineering, University of Pretoria, Pretoria, South Africa
[d] Department of Medical Research, China Medical University Hospital, China Medical University, Taichung, 404, Taiwan
[e] Department of Chemistry, Covenant University, Ota, Nigeria

ARTICLE INFO

Keywords:
Aluminum sulfate
Magnesium sulfate
Mono nanofluid
Heat transfer
Hybrid nanofluid
Radiator

ABSTRACT

The paper investigates the heat transfer performance of distilled water (DW) and ethylene glycol-DW mixture (EG-DW) based aluminum and magnesium sulfate nanofluids and their hybrid nanofluids in a radiator. Mono and hybrid nanofluids at 0.05% and 1% volume fractions with Malay Apple (Syzygium Malaccense) extract were formulated and run in the experimental set up at 0.4 kg/s. The heat transfer performances of DW, EG-DW, mono, and hybrid nanofluids were determined using Nusselt number (*Nu*), heat transfer rate ($\dot{Q}$) and coefficient (h), effectiveness (ε), heat transfer (Q), Prandtl number (Pr). An increment in the volume fraction was found to enhance $\dot{Q}$, h, *Nu*, Q, Pr, and ε. The maximum heat transfer performance was obtained using mono (Mg/DW (Q = 2.26 kW and *Nu* = 175), Al/EG-DW (Q = 6.57 kW and *Nu* = 462)) and hybrid (Mg–Al/DW (Q = 10.06 kW and *Nu* = 348)) nanofluids. In comparison with the corresponding base fluid, maximum heat transfer enhancements of 13.9%, 306.7%, and 493.9% were obtained for Mg/DW, Mg–Al/DW, and Al/EG-DW nanofluids, respectively. This remarkable heat transfer enhancement obtained can be related to the presence of the Malay Apple (Syzygium Malaccense) extract. These novel nanofluids appeared to be suitable candidates for radiator cooling.

1. Introduction

Internal combustion engines produce huge amounts of heat while running, and this can result in component damage and engine failure. Thus, the role of the cooling system in an automobile vehicle is crucial. Radiators (as heat exchangers) play a vital role in this regard as they remove excess heat from the engine. So, increasing the efficiency of a radiator also increases the engine life of the automobile, and this can be achieved via air and liquid (water, ethylene glycol (EG), water + EG, oils) cooling [1]. These cooling techniques with the incorporation of surface modification (fins and tubes) and expansion have been reported to have reached their practicable limits in attempts to enhance the efficiency of radiators [2,3]. Nanofluids obtained by the dispersion of nanoparticles (mono and hybrid) in thermal fluids have been extensively studied for heat and mass transfer in different thermal devices [4–11]. The

* Corresponding author. Mechanical Engineering Department, Covenant University, Ota, Nigeria.
** Corresponding author. Department of Mechanical and Aeronautical Engineering, University of Pretoria, Pretoria, South Africa.
E-mail addresses: sunday.oyedepo@covenantuniversity.edu.ng (S.O. Oyedepo), mohsen.sharifpur@up.ac.za (M. Sharifpur).

https://doi.org/10.1016/j.csite.2021.101494
Received 8 June 2021; Received in revised form 15 September 2021; Accepted 25 September 2021
Available online 2 October 2021

Nomenclature

A	Surface area of pipe, m^2
Al	Aluminum sulfate ($Al_2(SO_4)_3$)
c_p	Specific heat capacity (at constant pressure), J/kg°C
D_h	Characteristic length of tube, m
DW	Distilled water
EG	Ethylene glycol
f	Friction factor
h	Coefficient of heat transfer, $W/m^{2\circ}C$
h_i	Inlet coefficient of heat transfer, $W/m^{2\circ}C$
h_o	Outlet coefficient of heat transfer, $W/m^{2\circ}C$
L	Length of pipe, m
$\dot{m}$	Mass flow rate, kg/s
M	Mass of nanoparticles' type, g
Mg	Magnesium sulfate ($MgSO_4$)
Nu	Nusselt number
Pe	Peclet number
Pr	Prandtl number
$\dot{Q}$	Heat transfer rate, W
r_1	Radius of inlet of pipe, m
r_2	Radius of outlet of pipe, m
Re	Reynolds number
T	Temperature, °C
U	Overall heat transfer coefficient, W/m^2 °C
V	Volume, m^3

Greek symbols

K	Thermal conductivity, W/m K
ρ	Density of nanoparticles, kg/m^3
ϕ	Volume concentration/total concentration
ϕ_v	Volume fraction
μ	Viscosity, mPas
Δ	Change
ε	Effectiveness (%)
δ	Partial change
ν	Dynamic viscosity, kg/m s
α	Thermal diffusivity, m^2s
∂	Partial derivative

Subscript

b	bulk
bf	base fluid
hnf	hybrid nanofluid
i	inlet
m	mixture
mnf	mono nanofluid
np	nanoparticles
o	outlet
w	wall

advent of nanofluids has spurred investigations into their applications as coolants in radiators to augment the effectiveness and compactness of radiators.

Nieh et al. [12] studied the use of EG-water based Al_2O_3 and TiO_2 as nano-coolants to improve the heat transfer performance of an air-cooled radiator system. The experiment was performed under a series of volumetric flow rates and temperatures and using different volume fractions to determine the heat transfer rate, pumping power, pressure drop, and efficiency factor. The results showed that the heat transfer capacity and efficiency of the nano-coolants were much greater than that of the EG-water mixture and that of the TiO_2-based nano-coolant was greater than Al_2O_3-based nano-coolant. The enhanced heat transfer capacity, pressure drop, pumping power, and efficiency were 25.6%, 6.1%, 2.5%, and 27.2%, respectively when compared with the EG-water mixture. The authors

expressed concern that pressure drop and pumping power were not significant.

Ramaraju et al. [13] have worked on enhancing the h in an automobile radiator using MWCNTs (Multi-wall carbon nanotube). They showed that there was an improvement in heat transfer by 30% when MWCNTs/EG-water nanofluid was used compared with the EG-water blend. Mehtre and Kore [14] have investigated heat transfer performance in a car radiator using water-based Al_2O_3 nanofluids (with volume fractions of 0.5, 1, and 1.5%) at flow rates of 50 l/h – 200 l/h, velocity of 3.8 m/s, and temperature of 40 °C–75 °C. Their results have shown an augmentation of heat transfer with a rise in the flow rate of the coolants. The $\dot{Q}$ also improved with air flow rate increment. The heat transfer enhancement attained was in the range of 19%–42% when compared with pure water. Deshpande et al. [15] have investigated the heat removal rate of nano-coolant in an automobile radiator. Water-based MWCNT nanofluid was employed to enhance heat removal rate from and off the engine to the radiator under varying temperatures (50–70 °C) and volume fractions. It was observed that at 50 °C, 32% thermal efficiency was recorded using 0.2% MWCNT. Dhale et al. [16] have studied the effect of Al_2O_3 nanofluids (volume fraction of 0–1.2%) on the cooling system of an engine. They observed that the efficiency of the automotive radiator was greatly enhanced up to the tune of 24% at a constant flow rate of 0.167 kg/s. Sathish and Manivel [17] have studied the performance of $AgNO_3$ nanofluids (0.05–0.2%) in a car radiator, experimentally. The overall heat transfer was noticed to improve with volume fraction. However, there was a decline in the heat transfer performance when the volume fraction was increased beyond 0.2% such as at 0.3%. This showed that 0.2% $AgNO_3$ nanofluid gave the best heat transfer performance under the assumed conditions.

Ali et al. [18] have done an experimental investigation of the convective heat transfer using ZnO/water nanofluids (volume fraction of 0.01–0.3%) as coolants in a radiator under a fluid flow rate of 7–11 L/min (Re of 17500–27600). The heat transfer enhancement of 46% was noticed for 0.2% volume fraction. When the 0.3% volume fraction sample was tested, there was a decline in the heat transfer enhancement with the inlet temperature of the fluid kept in the range of 45–55 °C, showing conformity with the work of [17]. Wani and Ravi [19] have conducted an experimental study and computational fluid dynamics analysis on the thermal performance parameter of a car radiator using MgO/water nanofluid. They demonstrated that using flow rates of 5–9 L/min and different volume fractions, the average heat transfer was enhanced by 40–70%. The experimental results were then validated using computational fluid dynamics techniques to check for temperature distribution across the radiator.

Hamad [20] has investigated the heat transfer performance of EG-DW-based CuO and TiO_2 nanofluids at different volume concentrations (0.5–5%) and particle sizes as working fluids in a radiator. The result has shown that there was an improvement in the various tested mixture blends. In comparison with EG-DW, 55% enhancement of the radiator efficiency was recorded with 5% CuO nanofluid whereas 47% was observed with 5% TiO_2 nanofluid. CuO/EG-DW nanofluids showed improved heat transfer performance than TiO_2/EG-DW due to the particle size and κ of CuO nanoparticles. Sheikhzadeh et al. [21] have performed an investigation on the use of Al_2O_3/EG-water nanofluids in a car radiator to examine the heat transfer performance. The experiment was performed at different volume fractions (0.003–0.012%) and flow rates (9–14 L/min). The results have shown that an improvement in the h and *Nu* with a steady increase in flow rate. Also, the h improved with a rise in the volume fraction of the nanofluid. Khan et al. [22] have studied the influence of volume concentration (0.01–0.04 vol%) and flow rate (4–12 l/min) on the heat transfer performance of ZnO/EG-water (50:50) nanofluids as coolants in a car radiator. They showed that enhancement of $\dot{Q}$ and overall h as the volume concentration increased. Peak augmentation of heat transfer (36%) was achieved with 0.04 vol% ZnO nanofluid. At minimum inlet temperature and low flow rates (4 L/min and 6 L/min), higher $\dot{Q}$ was noticed.

Tijani and Sudirman [23] have numerically investigated the heat transfer characteristics (in terms of κ, *Nu*, h, and $\dot{Q}$) of EG-water (50:50) based Al_2O_3 and CuO nanofluids with nanoparticle concentration of 0.05–0.3% in a radiator under flow rates of 3–6 L/min. They have observed that CuO nanofluids show a higher heat transfer performance than Al_2O_3 nanofluids. At a flow rate of 0.6 L/min and concentration of 0.3%, the $\dot{Q}$, *Nu*, and h of 28.45 W and 28.25 W, 208.71 and 173.19, and 36384.41 W/m^2 K and 31005.9 W/m^2 K were recorded for CuO and Al_2O_3 nanofluids, respectively, compared with EG-water having a h of 13145.95 W/m^2 K and *Nu* of 164.29. Palaniappan and Ramasamy [24] have examined the influence of flow rate and volume concentration (0.2–2 vol%) on the exergy performance (exergy efficiency and exergy destruction rate), energy transfer (performance index and pumping power), and heat transfer metrics ($\dot{Q}$ and overall h) of EG-water based fly ash nanofluids in a radiator under a Re range of 4000–8000. They have demonstrated that the heat transfer variables were considerably enhanced as the volume concentration of fly ash nanofluid increased. By increasing the Re from 4000 to 8000, the overall h and $\dot{Q}$ of 0.2 vol% fly ash nanofluid and EG-water were improved by 25.5% and 15.9% and 27.4% and 33.3%, respectively. In comparison with EG-water, the pumping power was enhanced by 50% for 2 vol% fly ash nanofluid at Re of 8000. A higher performance index was observed for fly ash nanofluids under increasing Re compared with the EG-water, whereas the exergy variables were lower for the nanofluids than the EG-water.

Due to intensified research and progress in nanofluid studies which led to the emergence of hybrid nanofluid as a superior thermal fluid to conventional fluid and mono nanofluid, researchers have ignited their interest in the formulation and investigation of hybrid nanofluids [25]. The hybrid nanofluids have shown improved thermal conductivity properties than the mono nanofluids. The deployment of hybrid nanofluids as coolants in radiators is very scarce in the open literature with very few studies in this regard [3, 26–30]. Soylu et al. [28] investigated the thermo-hydraulic (*h*, pressure gradient, pumping power, thermal performance factor, and effectiveness) performance of EG-water (50:50) based Ag (0.1 and 0.3%)-TiO_2 and Cu (0.1%)-TiO_2 nanofluids with $\phi = 0.3$–2 vol% as coolants in the radiator of an automobile. Under increasing flow rates (17–24 L/min) and laminar conditions, the authors have reported that the *h*, pressure gradient, and effectiveness were enhanced with flow rate and ϕ increase. At the flow rate of 19 L/min, peak *h* enhancements of 5.62% and 11.09% were observed for 0.1% Ag–TiO_2 and 0.3%Ag–TiO_2 nanofluids, respectively. The highest pumping power of 2.9% (maximum) was recorded in this study. The thermal performance factor and effectiveness of 0.1% Ag–TiO_2 and 0.3%Ag–TiO_2 nanofluids were noticed to satisfy >1 and 0.4–0.6 specifications, respectively.

Recently, Ramalingam et al. [29] have experimentally investigated the performance (*Nu*, pressure gradient, and friction factor) of EG-distilled water (50:50) based Al_2O_3–SiC (60:40 and 50:50) nanofluids with $\phi = 0.4$ vol% and 0.8 vol% as working fluids in a radiator under varying flow rates. The effect of milled and unmilled SiC material on the performance of the hybrid nanofluids in the radiator was also investigated. They observed that *Nu* and pressure gradient augmented as ϕ and the flow rate increased, whereas *f* decreased with a rise in Re as the flow rate surged. Highest *Nu* and lowest *f* were recorded for Al_2O_3–SiC nanofluids with milled SiC. *Nu* and *f* (at 65 °C) of 23.46% and 9.97% and 8.98% and 2.34% were observed for Al_2O_3–SiC (50:50) and Al_2O_3–SiC (60:40) nanofluids, at $\phi = 0.4$ vol% and 0.8 vol% respectively, when compared with EG-distilled water. Benedict et al. [30] have investigated thermal performance (h, *Nu*, Re, and $\dot{Q}$) of EG-distilled water-based crystalline nanocellulose (CNC) and Al_2O_3–CNC nanofluids (with volume concentration of 0.5 vol%) as coolants in a radiator under varying flow rates (3.5–5.5 l/min). Results have shown that *Nu*, Re, $\dot{Q}$ and h, and temperature of all samples improved as the flow rate increased. Except for Re (reverse), other parameters demonstrated an enhancement trend of Al_2O_3–CNC > CNC > EG-distilled water. At flow rates of 3.5–5.5 L/min, the h, *Nu*, and $\dot{Q}$ of 87.23–94.93 W/m^2 K, 21.86–24.57, and 835.38–880.42 W, 54.23–60.28 W/m^2 K, 15.66–18.34, and 704.32–763.29 W, and 40.02–45.84 W/m^2 K, 10.98–13.64, and 525.02–566.32 W were recorded for 0.5 vol% Al_2O_3–CNC nanofluid, 0.5 vol% CNC nanofluid, and EG-distilled water, respectively.

The high thermal performance of 0.5 vol% Al_2O_3–CNC nanofluid was strongly connected to its high c_p and κ. In addition, Ganesan et al. [31] and Sahoo et al. [32] have documented the blending of lemon and sugarcane juice (biological extract) with base fluids (water, EG-water, propylene glycol, propylene glycol-water) and the suspension of nanoparticles to formulate nanofluids as a passive method for enhancing the convective heat transfer of nanofluids in radiators.

Based on the survey of the literature, studies on mono and hybrid nanofluids comprise of $MgSO_4$ and $Al_2(SO_4)_3$ with plant extract-water and EG-water as base fluids as nano-coolants for car radiator application are very scanty. Hence, this study aimed at investigating experimentally the thermal performance ($\dot{Q}$, ε, *Nu*, and h) of an automotive radiator using novel mono and hybrid nanofluids as coolants. The focus of the study was to explore the effect of base fluids, volume fractions, mono ($MgSO_4$ and $Al_2(SO_4)_3$) nanofluids, and hybrid ($MgSO_4$–$Al_2(SO_4)_3$) nanofluids on the heat transfer performance of a car radiator.

2. Material and methods

2.1. Materials

The salts ($MgSO_4{\cdot}16H_2O$ and $Al_2(SO_4)_3{\cdot}7H_2O$) are used in this study. The DW and EG are also procured.

2.2. Extract preparation

In agreement with previous studies that utilized extracts from different plants to enhance the heat transfer performance of nanofluids, this work engages Malay Apple (Syzygium Malaccense) to achieve heat transfer enhancement [31,32]. Malay Apple extract has been reported to possess heat transfer improving capacity [33], thus it is used in this study. The leaves of the Malay Apple were collected from the plant in an open field and were dried under a confined space for one month. Then, it was sun-dried to remove the remaining moisture in the leaves, after which they were grounded into relatively fine particles for further use. After soaking the fine-grounded leaves for 2 weeks in methanol (250 ml) to remove chemical compounds (extract). A rotary evaporator was used to eliminate the methanol contained in the mixture. The obtained extract (left idle in rubber jars) was used in the preparation of mono and hybrid nanofluids.

2.3. Preparation of nanofluid

The novel salts ($MgSO_4{\cdot}16H_2O$ and $Al_2(SO_4)_3{\cdot}7H_2O$) were chosen owing to their intricate characteristics that suit the purpose of this study. A two-way process was used to formulate the mono and hybrid nanofluids. The appropriate weight of the salts (depending on whether mono or hybrid nanofluids were to be formulated) was measured using a weighing balance. The mono and hybrid nanofluids (at volume fractions of 0.05% and 1%) were formulated using DW and EG-DW as base fluids according to Equation (1). A mixing ratio of 1:1 was used for the DW-EG base fluid and hybrid nanofluid ($MgSO_4$: $Al_2(SO_4)_3$) on a volume and weight basis, respectively. For both $MgSO_4$ and $Al_2(SO_4)_3$, 1 M was measured and dissolved in 1000 ml of DW and EG-DW. The extract of Malay Apple (2 g) was added to the new solution and then agitated for 2 h at 40 °C using a magnetic stirrer. After stirring, the mixture was filtered using a filter paper to obtain a relatively pure solution. To better homogenize the solution and separate any other impurity contained in it, it was centrifuged (using a centrifuge machine) for 15 min at 4000 rev/min. The residue of the solution was discarded, and the remaining solution (mono or hybrid nanofluid) was collected to be used for the heat transfer experiments. For both the mono and hybrid nanofluids, they were observed for a month to be without sediment.

$$\phi_v = \frac{V_{np}}{V} = \frac{V_{np}}{V_{np} + V_{bf}} = \frac{\frac{M\phi_v}{\rho_{np}}}{\left(\frac{M\phi_m}{\rho_{np}} + \frac{M(1-\phi_m)}{\rho_{bf}}\right)} \tag{1}$$

The fluids used for the experiments were; DW and EG-DW and $Al_2(SO_4)_3$/DW, $Al_2(SO_4)_3$/EG-DW, $MgSO_4$/DW, $MgSO_4$/EG-DW, $MgSO_4$–$Al_2(SO_4)_3$/DW, and $MgSO_4$–$Al_2(SO_4)_3$/EG-DW nanofluids.

2.4. Experimentation

The list of materials used in the construction of the test rig is provided in Table 1. Schematic representation of the experimental setup is shown in Fig. 1. The test rig was designed in a way that it represents the automobile and also showing the movement of coolants across the essential parts of the system that needs cooling. It consists of several components such as a fan, thermocouples, boiling ring, flow meter, reservoir tank, control valves, centrifugal water pump, light-duty radiator, and other smaller elements for connecting the joint such as clips, tapes, metallic pipes, and flexible hoses. Four liters of each of the 14 samples were run in the experiments. A preliminary study of the experiments conducted for 60 min and measurements taken every 10 min showed that thermal stability occurred 40 min after the commencement of the experiment. Thus, each experiment was run for 40 min and the measurements were also taken at 40 min.

2.5. Estimation of thermal transfer parameters

In a bid to analyze the results generated experimentally, some computations were carried out using the general equations use for solving heat flow.

T_b is the bulk temperature and was taken as the average of the inlet and outlet temperatures of the fluid flowing through the radiator, and it is expressed as

$$T_b = \frac{T_i + T_o}{2} \tag{2}$$

T_w is the wall temperature which is the average of the temperature of the two surface thermocouples and is expressed as;

$$T_w = \frac{T_2 + T_3}{2} \tag{3}$$

The heat gain is calculated using Eq. (4);

$$\dot{Q} = \dot{m} c_p \Delta T \tag{4}$$

Mass flow rate of the working fluid is given as;

$$\dot{m} = \rho V \tag{5}$$

From Newton's law of cooling, heat transfer can be calculated using;

$$\dot{Q} = h A_s (T_b - T_w) \tag{6}$$

When Eqs. (4) and (6) were compared, h was obtained and expressed as;

$$h = \frac{\dot{m} C_p (T_1 - T_4)}{A(T_b - T_w)} \tag{7}$$

Estimation of Re, *Pe* and Pr were as follows;

$$Re = \frac{\rho V D_h}{\mu}, .Pe = \frac{V D_h}{\alpha}. \; Pr = \frac{V}{\alpha} \tag{8}$$

The ν was estimated from Eq. (9),

$$\nu = \frac{k}{\rho C_p} \tag{9}$$

Table 1
Material listings.

S/N	Materials	Specifications
1.	Water pump	0.37 kW, 2.6 A (maximum flow 42 l/min)
2.	Light-duty radiator (down-flow radiator)	Capacity: 1 litre Size: 340 mm x 365 mm x 24 mm
3.	Flowmeter	Standard analogue
4.	Thermocouple	Type k with range (−50 °C – 750 °C)
5.	Boiling ring	220–240 V (1500 W)
6.	Abro radiator coolant (ethylene glycol)	4 litres
7.	Pipes and hoses	Materials: metal and flexible rubber
8.	Clips	Standard
9.	OX fan	230 V–50 Hz, 120 W
10.	Frame and tank fabrication	Galvanized steel tank and mild steel frame
11.	Electrical wires and extension outlets	10 A, 220 V, 50/60 Hz

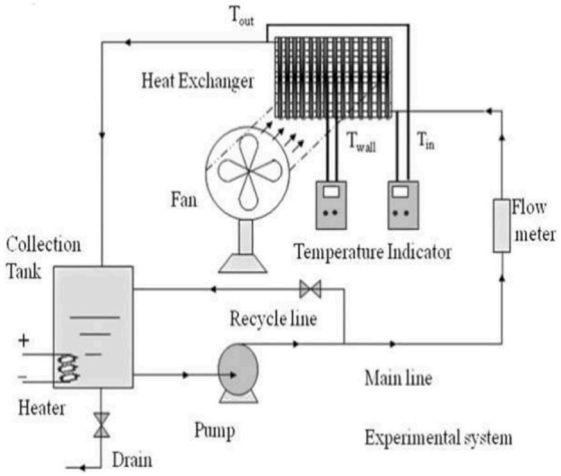

Fig. 1. Schematic representation of experimental setup.

The experimental *Nu* was expressed as:

$$Nu = \frac{hD_h}{k} \tag{10}$$

The overall h was given by Eq. (11);

$$\frac{1}{\mathrm{U}} = \left(\frac{1}{h_i A} + \frac{1}{2\pi kL} ln\frac{r_2}{r_1} + \frac{1}{h_o A}\right) \tag{11}$$

The heat transfer based on the overall h was estimated as

$$\dot{Q} = \mathrm{UA}\Delta\mathrm{T} \tag{12}$$

The friction factor was estimated using the following [30];

$$f = (0.79LnRe - 1.69)^{-2} \tag{13}$$

The percentage enhancement was obtained as

$$\text{Enhancement}\ \ (\%) = \frac{\mathrm{Nu_{mnf/hnf}} - \mathrm{Nu_{bf}}}{\mathrm{Nu_{bf}}} \times 100 \tag{14}$$

and the effectiveness was defined as

$$\varepsilon\ (\%) = \frac{\Delta T}{T_i} \times 100 \tag{15}$$

2.6. Data reduction process

The measured temperatures (using thermocouples) and the thermal properties of all the tested samples were engaged in the data reduction process. To calculate the various parameters such as Re, h, *Nu*, Pr as stated above in Equations (4) and (7)–9, and 11) for each tested sample, the thermal properties of the base fluids, mono, and hybrid nanofluids must first be estimated and thereafter substituted in the Equations. These thermal properties (κ, μ, c_p, and ρ) were estimated using Equations (16–23) [34–36].

$$k_{mnf} = k_{bf}\frac{k_{np} + 2k_{bf} - 2\phi\left(k_{bf} - k_{np}\right)}{k_{np} + 2k_{bf} + \phi\left(k_{bf} - k_{np}\right)} \tag{16}$$

$$k_{hnf} = k_{bf}\left(\frac{\left(\phi_{np1}k_{np1} + \phi_{np2}k_{np2}\right)}{\phi} + 2k_{bf} + 2\left(\phi_{np1}k_{np1} + \phi_{np2}k_{np2}\right) - 2\phi k_{bf}\right) \times \left(\frac{\left(\phi_{np1}k_{np1} + \phi_{np2}k_{np2}\right)}{\phi} + 2k_{bf} - \left(\phi_{np1}k_{np1} + \phi_{np2}k_{np2}\right) + \phi k_{bf}\right)^{-1} \tag{17}$$

$$\mu_{nf} = \frac{\mu_{bf}}{(1-\phi)^{2.5}} \tag{18}$$

$$\mu_{hnf} = \frac{\mu_{bf}}{\left(1 - \left(\phi_{np1} + \phi_{np2}\right)\right)^{2.5}} \tag{19}$$

$$\rho_{mnf} = (1-\phi)\rho_{bf} + \phi\rho_{np} \tag{20}$$

$$\rho_{hnf} = (1-\phi)\rho_{bf} + \phi_{np1}\rho_{np1} + \phi_{np2}\rho_{np2} \tag{21}$$

$$\left(\rho c_p\right)_{mnf} = (1-\phi)\left(\rho c_p\right)_{bf} + \phi\left(\rho c_p\right)_{np} \tag{22}$$

$$\left(\rho c_p\right)_{hnf} = (1-\phi)\left(\rho c_p\right)_{bf} + \phi_{np1}\left(\rho c_p\right)_{np1} + \phi_{np2}\left(\rho c_p\right)_{np2} \tag{23}$$

2.7. Uncertainty estimation

The sources of error in this study were principally from temperature and flow rate measurements. Accuracies of 0.75% (measured temperature) +1 °C and ±0.01% of full-scale flow rate +2% (measured value) were associated with the thermocouples and flow meter, respectively. These errors were propagated using Equations 24–28 to estimate the uncertainty of $\dot{m}$, $\dot{Q}$, *Nu*, h, and Re [9,10,34].

$$\delta\dot{m} = \left(\left(\frac{\partial\dot{m}}{\partial\rho}\delta\rho\right)^2 + \left(\frac{\partial\dot{m}}{\partial V}\delta V\right)^2\right)^{\frac{1}{2}} \tag{24}$$

$$\delta\dot{Q} = \left(\left(\frac{\partial\dot{Q}}{\partial\dot{m}}\delta\dot{m}\right)^2 + \left(\frac{\partial\dot{Q}}{\partial C_p}\delta c_p\right)^2 + \left(\frac{\partial\dot{Q}}{\partial\Delta T}\delta\Delta T\right)^2\right)^{\frac{1}{2}} \tag{25}$$

$$\delta h = \left(\left(\frac{\partial h}{\partial\dot{Q}}\delta\dot{Q}\right)^2 + \left(\frac{\partial h}{\partial A}\delta A\right)^2 + \left(\frac{\partial h}{\partial U}\delta U\right)^2\right)^{\frac{1}{2}} \tag{26}$$

$$\delta Nu = \left(\left(\frac{\partial Nu}{\partial h}\delta h\right)^2 + \left(\frac{\partial\dot{Q}}{\partial D_h}\delta D_h\right)^2 + \left(\frac{\partial\dot{Q}}{\partial\kappa}\delta\kappa\right)^2\right)^{\frac{1}{2}} \tag{27}$$

$$\delta Re = \left(\left(\frac{\partial Re}{\partial\rho}\delta\rho\right)^2 + \left(\frac{\partial Re}{\partial D_h}\delta D_h\right)^2 + \left(\frac{\partial Re}{\partial\mu}\delta\mu\right)^2 + \left(\frac{\partial Re}{\partial V}\delta V\right)^2\right)^{\frac{1}{2}} \tag{28}$$

Maximum uncertainties of 1.42%, 5.57%, 4.13%, 4.25%, and 3.15% are estimated for $\dot{m}$, $\dot{Q}$, *Nu*, h, and Re, respectively, using the relevant equations.

3. Results and discussion

3.1. Thermophysical properties of tested samples

Using Equations (16–23), the thermal properties (c_p, κ, ρ, and μ) of DW, EG-DW, mono ($MgSO_4$, and $Al_2(SO_4)_3$) nanofluids and hybrid nanofluids ($MgSO_4$–$Al_2(SO_4)_3$) are estimated and presented in Table 2. In this study, the $MgSO_4$, $Al_2(SO_4)_3$, and

Table 2
Thermophysical properties of hybrid and mono nanofluids and base fluids.

c_p (J/kg °C)	ρ (kg/m^3)	μ x 10^{-4} (Pas)	κ (W/m °C)	Sample
4125.8	999.1	7.08	0.6291	Mg–Al/DW (1%)
4163.7	991.4	6.91	0.6252	Mg–Al/DW (0.05%)
3181.7	1068.9	24.43	0.3789	Mg–Al/EG-DW (1%)
3202.6	1061.5	23.63	0.3786	Mg–Al/EGDW (0.05%)
3177.6	1068.9	25.27	0.3786	Mg/EG-DW (1%)
3202.4	1061.8	23.86	0.3778	Mg/EG-DW (0.05%)
3185.8	1070.5	25.93	0.3789	Al//EG-DW (1%)
3235.1	1051.3	23.57	0.3773	Al/EG-DW (0.05%)
4121.7	999.8	7.45	0.6302	Mg/DW (1%)
4163.5	990.8	6.82	0.6236	Mg/DW (0.05%)
4126.0	1000.7	7.50	0.6243	Al//DW (1%)
4162.7	993.7	7.34	0.6220	Al/DW (0.05%)
4165.7	993.5	7.36	0.6240	DW
3350.8	1064.3	25.56	0.3768	DW-EG

$MgSO_4$–$Al_2(SO_4)_3$ nanofluids are denoted as Mg, Al, and Mg–Al, respectively. From Table 2, it can be observed that κ, ρ, and μ of mono and hybrid nanofluids are enhanced as volume fraction rises from 0.05% to 1%. However, a reduction in ρ with an increase in volume fraction is noticed for the mono and hybrid nanofluids. These observations are found to agree with the literature concerning the influence of volume fraction on these thermal properties for mono and hybrid nanofluids [37–43].

3.2. Temperature profile of the experiment

Table 3 presents the temperature profile of the experiment in terms of the bulk and wall temperatures. The base fluid composed of EG-DW is noticed to have a relatively higher bulk and wall temperature than DW. Similarly, the bulk and wall temperatures of the DW-based mono and hybrid nanofluids are lower than those of EG-DW based mono and hybrid nanofluids. This characteristic could be strongly linked to the type and thermal properties of base fluid engaged in the experiment. In addition, it is generally noticed that the increase in the volume fractions of both the mono and hybrid nanofluids of Al and Mg resulted in a slight reduction in both the bulk and wall temperatures. This shows that increasing the quantity of Al, Mg, and Mg–Al nanoparticles dispersed into the respective base fluid enhances the overall temperature of the system, which agreed with previous studies [9,22,29].

3.3. Thermal performance of mono nanofluids

3.3.1. With DW as a base fluid

Subject to the experimental runs and reduction of data, values of $\dot{Q}$, h, *f*, *Pe*, Pr, *Nu*, Re, and ε are obtained for DW, EG-DW, mono, and hybrid nanofluids of DW and EG-DW base fluids as presented in Table 4. For DW-based mono nanofluids, it is noticed that $\dot{Q}$, h, *f*, Pr, *Nu*, and ε values increase as the volume fraction rises from 0.05% to 1%, whereas the reverse is observed for Re and *Pe* [44,45]. Except for Pr Number, the $\dot{Q}$, h, *f*, *Pe*, *Nu*, Re, and ε of DW are higher than those of EG-DW.

From Table 4, it can be noticed that at the respective volume fraction, Mg nanofluid yields higher *Nu* and Re than Al nanofluid. It is observed that increasing the volume fraction of Mg and Al nanofluids enhance *Nu* but decrease Re. This is found to agree with the literature [22,44,45]. The *Nu* (175.1) of 1% Mg/DW nanofluid is higher than those of other nanofluids and DW. From Table 4, the *Nu* (153.8) of DW found to be higher than those of Al/DW (0.05% and 1%) and Mg (0.05%) nanofluids. Thus, no heat transfer is recorded using Al/DW (0.05% and 1%) and Mg (0.05%) nanofluids. Also, Re is found to reduce from 18.2 to 16.7 (Mg/DW nanofluid) and 16.9 to 16.5 (Al/DW nanofluid) as volume fraction increased from 0.05% to 1%. This is due to the reduction in flow rate as the increased dispersion of the Mg and Al nanoparticles enhanced the μ of the mono nanofluids.

For the h and $\dot{Q}$ of mono nanofluids of Al and Mg, increasing the volume fraction of Al and Mg nanofluids from 0.05% to 1% was noticed to enhance h and $\dot{Q}$(see Table 4). The maximum $\dot{Q}$, (2.26 kW) and h (3522 W/m^2 °C) were achieved using 1% Mg/DW nanofluid. This agreed with previous studies found in the literature [19,21]. From Table 4, it can be observed that the $\dot{Q}$, (2.61 kW) and h (3095–3522 W/m^2 °C) of DW were greater than those of Al/DW (1% and 0.05%) and Mg/DW (0.05%) nanofluids. This implied heat transfer deterioration using these mono nanofluids.

3.3.2. With EG-DW as a base fluid

From Table 4, it can be noticed that $\dot{Q}$, h, Pr, *Nu*, and ε improved as the volume fraction of EG-DW based mono nanofluids increased. The opposite was found with Re, *f*, and *Pe* as volume fraction surged from 0.05% to 1%. The table equally revealed higher values of $\dot{Q}$, *Pe*, h, *f*, Pr, *Nu*, and ε for EG-DW mono nanofluids compared to those of DW-based mono nanofluids. The thermal properties of EG-DW could be responsible for these results. *Nu* of Al/EG-DW nanofluids was higher than those of Mg/EG-DW nanofluids with the lowest recorded for EG-DW. Increasing volume fraction was noticed to reduce Re for these mono nanofluids. It can be noticed in Table 4 that by increasing the volume fraction, *Nu* was enhanced for the EG-DW based Al and Mg nanofluids. *Nu* of 462.0, 352.4, 290.0, and 227.3 was obtained for EG-DW based 1% Al, 0.05% Al, 1% Mg, and 0.05% Mg nanofluids, respectively. These values were higher than those reported in the literature [22,46]. With EG-DW recording the lowest *Nu* (78.5) compared with the mono nanofluids, it was evident that these nanofluids enhanced heat transfer. However, Benedict et al. [30] showed that with EG-DW (60:40) based hybrid (Al_2O_3–CNC) and mono (CNC) nanofluids deployed to study their performance in a car radiator, *Nu* of 21.86–24.57 and 15.66–18.34 respectively were recorded, which were lower than the *Nu* values obtained in this work.

Considering Table 4, it can be noticed that the *Nu* of EG-DW nanofluids was considerably higher than those of DW-based nanofluids. In addition, the Re of DW-based nanofluids was more than those of EG-DW nanofluids. $\dot{Q}$ and h of 6.57 kW and 5.09 kW and 5622 W/

Table 3
Temperature profile of experiment.

Temperature (°C)	Base fluid	Mg (1 vol%)	Mg (0.05 vol%)	Al (1 vol%)	Al (0.05 vol%)	Mg–Al (1 vol%)	Mg–Al (0.05 vol%)
DW as base fluid							
Bulk temperature	35.5	36.65	41.8	36	35.9	38.75	40.7
Wall temperature	35.3	36.35	41.55	35.75	35.7	38.5	40.45
EG-DW as base fluid							
Bulk temperature	38.15	40.5	42.6	37.35	43.35	41.35	43.35
Wall temperature	38.05	40.2	42.35	37.1	43.1	41.05	43.1

Table 4
Heat transfer variables of hybrid and mono nanofluids and base fluids.

$\dot{Q}$ (W)	h (W/m^2 °C)	*Nu*	Re	Pr	*Pe*	ε (%)	*f*	Sample (%)
Hybrid nanofluid								
9076.7	7025.3	348.4	17.5	4.7	82.1	13.3	3.1	Mg–Al/DW (1)
4330.3	3351.6	165.2	17.9	4.6	81.8	6.2	2.9	Mg–Al/DW (0.05)
4227.4	3900.8	319.4	5.1	20.5	104.8	7.7	6.0	Mg–Al/EG-DW (1)
4199.9	3272.0	267.7	5.2	20.0	104.2	7.3	6.9	Mg–Al/EG-DW (0.05)
Mono nanofluid with EG-DW base fluid								
3813.2	3541.7	289.9	4.9	21.2	104.1	7.1	5.8	Mg (1)
3586.7	2776.1	227.3	5.2	20.2	104.9	6.4	6.6	Mg (0.05)
7263.6	5622.0	462.0	4.8	21.9	104.7	20.9	4.9	Al (1)
5564.3	4306.8	352.4	5.3	20.1	105.7	9.5	7.0	Al (0.05)
Mono nanofluid with DW base fluid								
3792.0	3522.0	175.1	16.7	4.9	82.0	6.1	3.5	Mg (1)
2970.7	2062.4	101.5	18.2	4.5	81.9	3.8	2.8	Mg (0.05)
3330.2	2577.5	128.5	16.5	5.0	83.0	5.4	3.6	Al (1)
2664.6	1839.5	91.3	16.9	4.8	82.0	4.9	3.4	Al (0.05)
Base fluids								
4998.9	3095.3	153.8	16.8	4.9	82.8	8.1	3.4	DW
3082.7	954.4	78.5	5.2	13.7	71.1	5.9	6.7	DW-EG

m^2 °C and 4306 W/m^2 °C were obtained for 1% and 0.05% Al/EG-DW nanofluids, respectively (Table 4). For Mg/EG-DW nanofluids, $\dot{Q}$ of 2.96 kW and 2.20 kW and h of 3542 W/m^2 °C and 2776 W/m^2 °C were recorded at volume fractions of 1% and 0.05%, respectively. These $\dot{Q}$ values were lower and h values were higher than that reported in the literature, though at higher Re and volume fraction [24]. With the use of EG-DW yielding $\dot{Q}$ of 646.2 W and h of 954.4 W/m^2 °C, heat transfer enhancement was experienced with the utilization of EG-DW based Al and Mg nanofluids. By comparing (in Table 4), it can be deduced that EG-DW based nanofluids produced higher $\dot{Q}$ and h compared to DW-based nanofluids. Better still, the use of EG-DW as base fluid favored improved heat transfer of Al and Mg nanofluids as thermal fluids in a car radiator.

3.4. Thermal performance of hybrid nanofluids

The values of $\dot{Q}$, h, *Nu*, Re, and ε for the DW-based hybrid nanofluids of Al and Mg were observed to be more than those of EG-DW hybrid nanofluids (Table 4). This was ably influenced by the thermal properties of the base fluid (DW). For both types of hybrid nanofluids, $\dot{Q}$, h, *Pe*, Pr, *Nu*, and ε were improved with an increase in volume fraction. However, the reverse was noticed for Re. The *f* value for DW-based hybrid nanofluids increased with volume fraction while that of EG-DW hybrid nanofluids reduced as volume fraction surged. At a specific volume fraction, the *Nu* of DW-based hybrid nanofluids was more than that of EG-DW hybrid nanofluids. The Re of Mg–Al/DW nanofluids was lower than the Re of Mg–Al/EG-DW nanofluids, which were observed to be identical to that of DW and EG-DW, respectively (Table 4). The *Nu* of 1% Mg–Al/DW, 0.05% Mg–Al/DW, 1% Mg–Al/EG-DW, and 0.05 Mg–Al/EG-DW nanofluids was 348.4, 165.2, 319.4, and 267.7, respectively, with that of DW = 153.8 and EG-DW = 78.5. This showed that 1% Mg–Al/DW nanofluid has the highest *Nu* value and that heat transfer enhancement was observed for both types of hybrid nanofluid in comparison with the respective base fluid. The *Nu* values were observed to be higher than those reported in the literature for hybrid

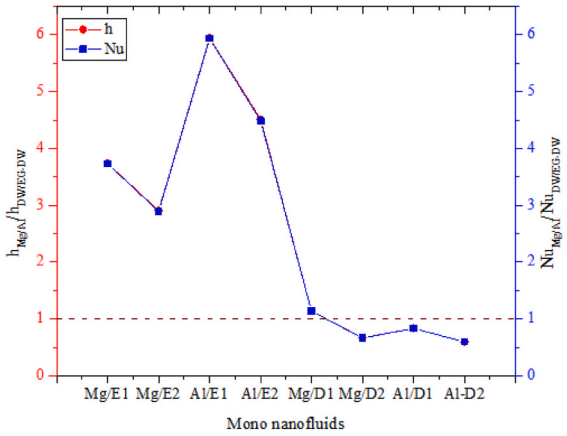

Fig. 2. Plot of normalized h and *Nu* against mono nanofluids (Note: E connotes EG-DW, D connotes DW while 1 and 2 represent volume fractions of 1% and 0.05% respectively).

nanofluids [29,32].

Similar to *Nu* (Table 4), the 1% Mg–Al/DW nanofluid produced the highest $\dot{Q}$ (10.06 kW) and h (7025.3 W/m^2 °C). The use of 0.05% Mg–Al/DW, 1% Mg–Al/EG-DW, and 0.05% Mg–Al/EG-DW nanofluids yielded 2.44 kW and 3351.6 W/m^2 °C, 3.56 kW and 3900.8 W/m^2 °C, and 3.03 kW and 3272 W/m^2 °C, respectively. The obtained $\dot{Q}$ was noticed to be slightly lower while the h was moderately higher than those reported in previous studies [28,32]. In comparison with the base fluids (DW ($\dot{Q}$ = 2.61 kW and h = 3095 W/m^2 °C) and EG-DW ($\dot{Q}$ = 646.2 kW and h = 954.4 W/m^2 °C)), both types of hybrid nanofluids demonstrated improvement in heat transfer.

3.5. Enhancement and effectiveness of mono and hybrid nanofluids

3.5.1. Enhancement

Based on Equation (14), both the *Nu* and h enhancement afforded by utilizing DW and EG-DW based mono and hybrid nanofluids as nano-coolants in a car radiator were estimated. Fig. 2 illustrates the normalized *Nu* and h against the DW and EG-DW nanofluids. It can be deduced from Fig. 2 that only five of the eight tested nanofluid samples showed heat transfer enhancement based on *Nu* and h when compared with the respective base fluid. Heat transfer enhancement order of 1% Al/EG-DW > 0.05% Al/EG-DW > 1% Mg/EG-DW > 0.05% Mg/EG-DW > 1% Mg/DW was observed in this present study. This led to *Nu* enhancements of 493.9%, 348.8%, 269.2%, 189.5%, and 13.9% for 1% Al/EG-DW, 0.05% Al/EG-DW, 1% Mg/EG-DW, 0.05% Mg/EG-DW, and 1% Mg/DW nanofluids, respectively, in comparison with corresponding base fluid. This revealed that 1% Al/EG-DW nanofluid offered the maximum heat transfer.

With Fig. 3 displaying the normalized *Nu* and h for the DW and EG-DW based hybrid nanofluids, all the hybrid nanofluids were found to enhance heat transfer when engaged as nano-coolants in a car radiator. An order of 1% Mg–Al/EG-DW > 0.05% Mg–Al/EG-DW > 1% Mg–Al/DW > 0.05% Mg–Al/DW was noticed for the heat transfer afforded by the hybrid nanofluids. *Nu* was estimated to be enhanced by 306.7%, 240.9%, 126.6%, and 7.4% for 1% Mg–Al/EG-DW, 0.05% Mg–Al/EG-DW, 1% Mg–Al/DW, and 0.05% Mg–Al/DW nanofluids, respectively, when compared with the respective base fluid. This is an indication that the highest heat transfer improvement was obtained using 1% Mg–Al/EG-DW nanofluid. The above results showed that the deployment of EG-DW to formulate mono and hybrid nanofluid produced improved heat transfer in the car radiator compared with the use of DW. In addition, a recent review work by Abbas et al. [3] on the performance of nanofluids in car radiators reported that heat transfer, h, and *Nu* enhancements of 4.7%–90%, 10%–78.7%, and 3.4%–88% respectively, are achieved by engaging nanofluids as thermal fluids in car radiators. This revealed that most of the tested samples (mono and hybrid nanofluids) in this present work performed better than previous studies. This improvement in heat transfer can be linked to the use of Malay apple extract.

Furthermore, Benedict et al. [30] reported maximum values of 15.35% and 55.46% ($\dot{Q}$), 35.51% and 117.96% (h), and 34.46% and 80.13% (*Nu*) for mono (CNC) and hybrid (Al_2O_3–CNC) nanofluids, respectively, studied as thermal fluids in a radiator. Again, these metrics were found to be lower than the peak recorded for both mono and hybrid nanofluids studied in this present work. The normalized h values obtained in this work (mono and hybrid nanofluids) were noticed to be slightly higher than that found in the literature [28]. The hybridization of Mg and Al nanoparticles to formulate hybrid nanofluids using EG-DW was observed to augment the heat transfer capacity of 1% Mg/EG-DW nanofluid. It is worth mentioning that the remarkable enhancement of heat transfer exhibited by mono (1% Al/EG-DW, 0.05% Al/EG-DW, 1% Mg/EG-DW and 0.05% Mg/EG-DW) and hybrid (1% Mg–Al/EG-DW, 0.05% Mg–Al/EG-DW, 1% Mg–Al/DW) nanofluids were strongly connected to the utilization of Malay apple extract (bio-compounds) known to possess heat transfer augmentation capability.

3.5.2. Effectiveness

Table 4 presents the ε of DW-based mono nanofluids. Values of 6.1%, 3.8%, 5.4%, 4.9%, and 8.1% were obtained for 1% Mg/DW, 0.05% Mg/DW, 1% Al/DW, 0.05% Al/DW, and DW, respectively. The use of 1% Mg/DW nanofluid in the radiator produced the highest ε for DW-based mono nanofluids, which was consistent with those of *Nu*, Q, h, and $\dot{Q}$ earlier reported in this present study. From Table 4, the highest ε (20.9%) was obtained using 1% Al/EG-DW nanofluids. This finding was similar to those of *Nu*, Q, h, and $\dot{Q}$ mentioned above. The obtained values of ε for 0.05% Al/EGDW, 1% Mg/EG-DW, 0.05% Mg/EG-DW, and EG-DW were 9.5%, 7.1%, 6.4%, and 5.9%, respectively. The ε of the hybrid nanofluids engaged as coolants in the radiator is presented in Table 4. The ε of 1% Mg–Al/DW, 0.05% Mg–Al/DW, 1% Mg–Al/EG-DW, and 0.05% Mg–Al/EG-DW nanofluids was 13.3%, 6.2%, 7.7%, and 7.1%, respectively. This showed that peak ε was achieved using 1% Mg–Al/DW nanofluid, which agreed with other studied thermal metrics. It can be generally deduced that the obtained *Nu*, Q, h, and $\dot{Q}$ were strongly related to the volume fraction, base fluid and nanoparticles type, and hybridization of nanoparticles. The values of ε obtained in this study were noticed to be moderately lower than those reported for hybrid nanofluids of Al_2O_3 + TiO_2, + CuO, + SiC, + Cu, + AG [24] and higher than (0.33–0.41) stated in the literature for 0.3% Ag + TiO_2 nanofluid [28]. This is attributable to the lower κ of the nanofluids (Al, Mg, and Mg–Al) used in this present work.

4. Conclusion

Malay Apple extracts doped DW and EG-DW based mono, and hybrid nanofluids (with volume fractions of 0.05% and 1%) of Al and Mg nanoparticles are formulated using a two-step strategy and employed to investigate the heat transfer performance in a car radiator. With the stable mono and hybrid nanofluids and base fluids of DW and EG-DW, the $\dot{Q}$, h, *Nu*, Q, Pr, and ε were found to enhance as nanoparticles increased due to volume fraction increment. In addition, the EG-DW and the EG-DW based mono and hybrid nanofluids

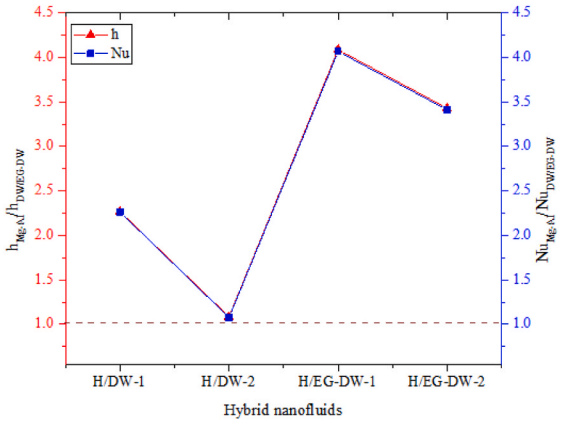

Fig. 3. Plot of normalized h and *Nu* against hybrid nanofluids (Note: 1 and 2 represent volume fractions of 1% and 0.05% respectively).

show higher bulk and wall temperatures compared with the DW and DW-based mono and hybrid nanofluids. The highest heat transfer is recorded with the use of Mg/DW ($\dot{Q} = 3.79$ kW and $Nu = 175$), Al/EG-DW ($\dot{Q} = 7.26$ kW and $Nu = 462$), and Mg–Al/DW ($\dot{Q} = 9.07$ kW and $Nu = 348$) nanofluids (as mono and hybrid types). Similar trends were observed for the h and ε of these mono and hybrid nanofluids. In comparison with the respective base fluids, heat transfer enhancements of 13.9%, 306.7%, and 493.9% were obtained for Mg/DW, Mg–Al/DW, and Al/EG-DW nanofluids, respectively. The presence of the Malay apple extract was observed to be responsible for the significant heat transfer enhancement reported in this work. The deployment of EG-DW as base fluid was noticed to favor heat transfer augmentation owing to the relatively low κ of Al and Mg nanoparticles and EG-DW while hybridizing nanoparticles favored heat transfer for DW as thermal fluid.

Authors' Statement (Contributions)

Kelvin U. Efemwenkiekie - Conception, experimental set-up and writing of the first draft.
Sunday O. Oyedepo – Supervision of the project, reading, reviewing and editing.
Solomon O. Giwa– Reading, reviewing and editing.
Mohsen Sharifpur – Reading, reviewing and editing, as well as funding open access.
Taiwo F. Owoeye – Experimental set-up.
Kehinde D. Akinlabu – Experimental set-up.
Josua P. Meyer – Reading, reviewing and editing.

Declaration of competing interest

The authors declare that they have no known competing financial interests or personal relationships that could have appeared to influence the work reported in this paper.

References

[1] U.K. Efemwenkiekie, S.O. Oyedepo, U.D. Idiku, D.C. Uguru-Okorie, A. Kuhe, Comparative analysis of a four stroke spark ignition engine performance using local ethanol and gasoline blends, Procedia Manuf. 35 (2019) 1079–1086.
[2] S.O. Giwa, M. Sharifpur, M.H. Ahmadi, J.P. Meyer, A review of magnetic field influence on natural convection heat transfer performance of nanofluids in square cavities, J. Therm. Anal. Calorim. (2020), https://doi.org/10.1007/s10973-020-09832-3.
[3] F. Abbas, H.M. Ali, T.R. Shah, H. Babar, M.M. Janjua, U. Sajjad, M. Amer, Nanofluid: potential evaluation in automotive radiator, J. Mol. Liq. 297 (2020) 112014.
[4] L. Cheng, M. Nawaz, H. Kaneez, M.K. Alaoui, A. Selmi, C. Li, H. Assilzadeh, Flow and heat transfer analysis of elastoviscoplastic generalized non-Newtonian fluid with hybrid nano structures and dust particles, Int. Commun. Heat Mass Tran. 126 (2021), https://doi.org/10.1016/j.icheatmasstransfer.2021.105275.
[5] I. Haider, U. Nazir, M. Nawaz, S.O. Alharbi, I. Khan, Numerical thermal study on performance of hybrid nano-Williamson fluid with memory effects using novel heat flux model, Case Stud. Therm. Eng. 26 (2021) 101070, https://doi.org/10.1016/j.csite.2021.101070.
[6] M. Nawaz, H.A. Madkhali, M. Haneef, S.O. Alharbi, M.K. Alaoui, Numerical study on thermal enhancement in hyperbolic tangent fluid with dust and hybrid nanoparticles, Int. Commun. Heat Mass Tran. 127 (2021), https://doi.org/10.1016/j.icheatmasstransfer.2021.105535.
[7] H.A. Madkhali, M. Nawaz, S.O. Alharbi, Y. Elmasry, An enhancement of energy transport and mass in hybrid nanofluid under magnetic field and temperature and mass concentration gradients, Case Stud. Therm. Eng. 27 (2021) 101182, https://doi.org/10.1016/j.csite.2021.101182.
[8] P.K. Kanti, K.V. Sharma, A.A. Minea, V. Kesti, Experimental and computational determination of heat transfer, entropy generation and pressure drop under turbulent flow in a tube with fly ash-Cu hybrid nanofluid, Int. J. Therm. Sci. 167 (2021) 107016.
[9] L.S. Sundar, A.H. Misganaw, M.K. Singh, A.M.B. Pereira, A.C.M. Sousa, Efficiency, energy and economic analysis of twisted tape inserts in a thermosyphon solar flat plate collector with Cu nanofluids, Renew. Energy Focus. 35 (2020) 10–31, https://doi.org/10.1016/j.ref.2020.06.004.
[10] S.O. Giwa, M. Sharifpur, J.P. Meyer, Experimental investigation into heat transfer performance of water-based magnetic hybrid nanofluids in a rectangular cavity exposed to magnetic excitation, Int. Commun. Heat Mass Tran. 116 (2020) 104698, https://doi.org/10.1016/j.icheatmasstransfer.2020.104698.
[11] C. Nwaokocha, M. Momin, S. Giwa, M. Sharifpur, S.M. Murshed, J.P. Meyer, Experimental investigation of thermo-convection behaviour of aqueous binary nanofluids of MgO-ZnO in a square cavity, Case Stud. Therm. Eng. (2021).

[12] H.M. Nieh, T.P. Teng, C.C. Yu, Enhanced heat dissipation of a radiator using oxide nano-coolant, Int. J. Therm. Sci. 77 (2014) 252–261.
[13] R.V. Ramaraju, M. Kota, H.B. Manap, V.R. Veeredhi, Enhancement of Heat Transfer Coefficient in an Automobile Radiator Using Multi Walled Carbon Nano Tubes (MWCNTS), American Society of Mechanical Engineers, International Mechanical Engineering Congress and Exposition, 2014, pp. 1–9. IMECE2014-36964.
[14] D.N. Mehtre, S.S. Kore, Experimental analysis of heat transfer from car radiator using nano-fluids, Int. J. Mech. Comput. Appl. 2 (4) (2014) 101–106.
[15] A. Deshpande, V. Patil, R. Patil, Experimental analysis of automobile radiator using MWCNT-water nanofluid, Int. J. Eng. Res. Technol. 5 (11) (2016) 97–101.
[16] P. Dhale, B. Wadhave, V. Kanade, S. Sable, Effect of nanofluid on cooling system of engine, Int. J. Eng. Appl. Sci. 2 (10) (2015) 8–10.
[17] S. Sathish, R. Manivel, Experimental investigation of automotive radiator using nanofluids, in: International Conference on Explorations and Innovations in Engineering & Technology, 2016, pp. 114–120. Wuhan China, held on March 26-27.
[18] H.M. Ali, H. Ali, H. Liaquat, H.T.B. Maqsood, M.A. Nadir, Experimental investigation of convective heat transfer augmentation for car radiator using ZnO–water nanofluids, Energy 84 (2015) 317–324.
[19] M.S.G. Wani, H.C. Ravi, Experimental study and CFD analysis of Thermal performance improvement of car radiator by MgO/water nanofluid, Int. Res. J. Eng. Technol. 4 (6) (2017) 1904–1911.
[20] A. Hamad, Experimental investigation of heat transfer in automobile radiator by using alternative working fluids and nanoparticles, Iraqi J. Mech. Matl. Engrg. 16 (4) (2016) 442–458.
[21] G.A. Sheikhzadeh, M.M. Fakhari, H. Khorasanizadeh, Experimental investigation of laminar convection heat transfer of Al_2O_3-ethylene glycol-water nanofluid as a coolant in a car radiator, J. Appl. Fluid Mech. 10 (1) (2017) 209–219.
[22] A. Khan, H.M. Ali, R. Nazir, R. Ali, A. Munir, B. Ahmad, Z. Ahmad, Experimental investigation of enhanced heat transfer of a car radiator using ZnO nanoparticles in H_2O–ethylene glycol mixture, J. Therm. Anal. Calorim. 138 (5) (2019) 3007–3020.
[23] A.S. Tijani, A.S. Bin Sudirman, Thermo-physical properties and heat transfer characteristics of water/anti-freezing and Al_2O_3/CuO based nanofluid as a coolant for car radiator, Int. J. Heat Mass Tran. 118 (2018) 48–57.
[24] B. Palaniappan, V. Ramasamy, Thermodynamic analysis of fly ash nanofluid for automobile (heavy vehicle) radiators, J. Therm. Anal. Calorim. 136 (1) (2019) 223–233.
[25] U.K. Efemwenkiekie, S.O. Oyedepo, Thermal conductivity of nanofluids in heat transfer applications–a review, J. Phys. Conf. 1378 (2019), 032074.
[26] B.R. Bharadwaj, K.S. Mogeraya, D.M. Manjunath, B.R. Ponangi, K.R. Prasad, V. Krishna, CFD analysis of heat transfer performance of graphene based hybrid nanofluid in radiators, Conf. Ser.: Mater. Sci. Eng. 346 (2017), 012084.
[27] A. Topuz, T. Engin, B. Erdoğan, S. Mert, A. Yeter, Experimental investigation of pressure drop and cooling performance of an automobile radiator using Al_2O_3-water + ethylene glycol nanofluid, Heat Mass Tran., https://doi.org/10.1007/s00231-020-02916-8.
[28] S.K. Soylu, İ. Atmaca, M. Asiltürk, A. Doğan, Improving heat transfer performance of an automobile radiator using Cu and Ag doped TiO_2 based nanofluids, Appl. Therm. Eng. 157 (2019) 113743.
[29] S. Ramalingam, R. Dhairiyasamy, M. Govindasamy, Assessment of Heat Transfer Characteristics and System Physiognomies Using Hybrid Nanofluids in an Automotive Radiator, Chemical Engineering and Processing-Process Intensification, 2020, p. 107886.
[30] F. Benedict, A. Kumar, K. Kadirgama, H.A. Mohammed, D. Ramasamy, M. Samykano, R. Saidur, Thermal performance of hybrid-inspired coolant for radiator application, Nanomaterials 10 (6) (2020) 1100.
[31] T. Ganesan, P. Seenikannan, T. Prabu, Effect of Al_2O_3 nanofluids with citrus limonum juice on heat transfer rate in automobile radiators, Int. J. Latest Eng. Res. Appl. 1 (2016) 86–102.
[32] R.R. Sahoo, P. Ghosh, J. Sarkar, Performance comparison of various coolants for louvered fin tube automotive radiator, Therm. Sci. 21 (2017) 2871–2881.
[33] R.C.I. Fontan, V.S. Sampaio, E.C. Souza Jr., R.G. Pereira, L.B. Rodrigues, G.R.F. Gonçalves, O.R.R. Gandolfi, R.C.F. Bonomo, Composition and thermophysical properties of Malay Rose Apple pulp, Int. Food Res. J. 25 (2018) 1067–1073.
[34] M. Sharifpur, S.O. Giwa, K.Y. Lee, H. Ghodsinezhad, J.P. Meyer, Experimental investigation into natural convection of zinc oxide/water nanofluids in a square cavity, Heat Tran. Eng. (2020) 1–13, https://doi.org/10.1080/01457632.2020.1818384, 0.
[35] M. Nawaz, U. Nazir, S. Obaid Alharbi, M. Kbiri Alaoui, Thermal and solutal analysis in power law fluid under non-Fourier's diffusion conditions, Int. Commun. Heat Mass Tran. 126 (2021), https://doi.org/10.1016/j.icheatmasstransfer.2021.105331.
[36] U. Nazir, N.H. Abu-Hamdeh, M. Nawaz, S.O. Alharbi, W. Khan, Numerical study of thermal and mass enhancement in the flow of Carreau-Yasuda fluid with hybrid nanoparticles, Case Stud. Therm. Eng. 27 (2021) 101256, https://doi.org/10.1016/j.csite.2021.101256.
[37] S.O. Giwa, M. Sharifpur, J.P. Meyer, S. Wongwises, O. Mahian, Experimental measurement of viscosity and electrical conductivity of water-based γ-Al_2O_3/MWCNT hybrid nanofluids with various particle mass ratios, J. Therm. Anal. Calorim. 143 (2021) 1037–1050.
[38] S.O. Giwa, M. Momin, C.N. Nwaokocha, M. Sharifpur, J.P. Meyer, Influence of nanoparticles size, per cent mass ratio, and temperature on the thermal properties of water-based MgO–ZnO nanofluid: an experimental approach, J. Therm. Anal. Calorim. 143 (2020) 1063–1079, 2021.
[39] S.M. Mousavi, F. Esmaeilzadeh, X.P. Wang, A detailed investigation on the thermo-physical and rheological behavior of MgO/TiO_2 aqueous dual hybrid nanofluid, J. Mol. Liq. 282 (2019) 323–339.
[40] M. Sharifpur, S. Yousefi, J.P. Meyer, A new model for density of nanofluids including nanolayer, Int. Commun. Heat Mass Tran. 78 (2016) 168–174.
[41] S.A. Adio, M. Mehrabi, M. Sharifpur, J.P. Meyer, Experimental investigation and model development for effective viscosity of MgO–ethylene glycol nanofluids by using dimensional analysis, FCM-ANFIS and GA-PNN techniques, Int. Commun. Heat Mass Tran. 72 (2016) 71–83.
[42] J. Ganeshkumar, D. Kathirkaman, K. Raja, V. Kumaresan, R. Velraj, Experimental study on density, thermal conductivity, specific heat, and viscosity of water-ethylene glycol mixture dispersed with carbon nanotubes, Therm. Sci. 21 (2017) 255–265.
[43] G. Żyła, J.P. Vallejo, J. Fal, L. Lugo, Nanodiamonds–ethylene glycol nanofluids: experimental investigation of fundamental physical properties, Int. J. Heat Mass Tran. 121 (2018) 1201–1213.
[44] L.S. Sundar, M.K. Singh, A.C. Sousa, Enhanced heat transfer and friction factor of MWCNT–Fe_3O_4/water hybrid nanofluids, Int. Commun. Heat Mass Tran. 52 (2014) 73–83.
[45] L.S. Sundar, M.K. Singh, A.C. Sousa, Turbulent heat transfer and friction factor of nanodiamond-nickel hybrid nanofluids flow in a tube: an experimental study, Int. J. Heat Mass Tran. 117 (2018) 223–234.
[46] S.M. Peyghambarzadeh, S.H. Hashemabadi, M.S. Jamnani, S.M. Hoseini, Improving the cooling performance of automobile radiator with Al_2O_3/water nanofluid, Appl. Therm. Eng. 31 (2011) 1833–1838.